Cannabinoid Type 1 Receptor Blockade Promotes Mitochondrial Biogenesis Through Endothelial Nitric Oxide Synthase Expression in White Adipocytes

Laura Tedesco,[1,2] Alessandra Valerio,[1,3] Cristina Cervino,[4] Annalisa Cardile,[1] Claudio Pagano,[5] Roberto Vettor,[5] Renato Pasquali,[4] Michele O. Carruba,[1,2] Giovanni Marsicano,[6] Beat Lutz,[7] Uberto Pagotto,[4] and Enzo Nisoli[1,2]

OBJECTIVE—Cannabinoid type 1 (CB1) receptor blockade decreases body weight and adiposity in obese subjects; however, the underlying mechanism is not yet fully understood. Nitric oxide (NO) produced by endothelial NO synthase (eNOS) induces mitochondrial biogenesis and function in adipocytes. This study was undertaken to test whether CB1 receptor blockade increases the espression of eNOS and mitochondrial biogenesis in white adipocytes.

RESEARCH DESIGN AND METHODS—We examined the effects on eNOS and mitochondrial biogenesis of selective pharmacological blockade of CB1 receptors by SR141716 (rimonabant) in mouse primary white adipocytes. We also examined eNOS expression and mitochondrial biogenesis in white adipose tissue (WAT) and isolated mature white adipocytes of CB1 receptor–deficient ($CB1^{-/-}$) and chronically SR141716-treated mice on either a standard or high-fat diet.

RESULTS—SR141716 treatment increased eNOS expression in cultured white adipocytes. Moreover, SR141716 increased mitochondrial DNA amount, mRNA levels of genes involved in mitochondrial biogenesis, and mitochondrial mass and function through eNOS induction, as demonstrated by reversal of SR141716 effects by small interfering RNA–mediated decrease in eNOS. While high-fat diet–fed wild-type mice showed reduced eNOS expression and mitochondrial biogenesis in WAT and isolated mature white adipocytes, genetic CB1 receptor deletion or chronic treatment with SR141716 restored these parameters to the levels observed in wild-type mice on the standard diet, an effect linked to the prevention of adiposity and body weight increase.

CONCLUSIONS—CB1 receptor blockade increases mitochondrial biogenesis in white adipocytes by inducing the expression of eNOS. This is linked to the prevention of high-fat diet–induced fat accumulation, without concomitant changes in food intake. ***Diabetes*** **57:2028–2036, 2008**

Adipose tissue is not merely an energy store but rather an endocrine organ playing an important role in fuel metabolism (1,2). Recent studies have demonstrated that mitochondrial biogenesis increases during adipocyte differentiation (3), and this is presumably due at least in part to the presence of the endothelial nitric oxide (NO) synthase (eNOS). In fact, eNOS protein is not expressed in either undifferentiated 3T3-L1 cells or preadipocytes, whereas its expression markedly increases with adipocyte differentiation (4). It is noteworthy that NO increases mitochondrial biogenesis in white adipocytes via cyclic guanosine monophosphate (cGMP)-dependent pathways, including peroxisome proliferator–activated receptor γ coactivator-1α (PGC-1α) gene expression (5,6). Consistently, mitochondrial biogenesis is reduced in fat of eNOS-null mutant mice ($eNOS^{-/-}$), with decreased energy expenditure and increased body weight (5,6). This suggests that the eNOS-dependent mitochondrial biogenesis is relevant to adipocyte maturation and fuel metabolism.

Cannabinoid type 1 (CB1) receptors participate in the physiological modulation of many central and peripheral functions related to the control of energy metabolism (7). They are the most abundant G protein–coupled receptors expressed in the brain, where CB1 receptor activation promotes feeding and modulates the rewarding properties of food (7–9). CB1 receptors also control metabolic functions by acting on peripheral organs, including white adipose tissue (WAT) (7–9). Notably, in adipocytes, CB1 receptor expression increases with cell differentiation (10,11). Moreover, CB1 receptor–deficient mice ($CB1^{-/-}$) are lean (12) and resistant to a high-fat diet (13). Similarly, the selective CB1 receptor antagonist SR141716 (rimonabant) persistently reduces body weight during the treatment of obese animals, although food intake renormalizes after an initial 1- to 2-week weight reduction (14,15), suggesting that CB1 receptor blockade stimulates fat metabolism, leading to a decreased fat content.

We now demonstrate a prominent role for the CB1 receptors to modulate eNOS gene expression and mitochondrial biogenesis in white adipocytes. Collectively, these data suggest that targeting the endocannabinoid system improves mitochondrial function, implying a novel,

From the [1]Integrated Laboratories Network, Center for Study and Research on Obesity, Department of Pharmacology, Chemotherapy and Medical Toxicology, School of Medicine, Milan University, Milan, Italy; the [2]Istituto Auxologico Italiano, Milan, Italy; the [3]Department of Biomedical Sciences and Biotechnologies, Brescia University, Brescia, Italy; the [4]Endocrinology Unit, Department of Internal Medicine and Gastroenterology, Center for Applied Biomedical Research, S. Orsola-Malpighi Hospital, Alma Mater Bologna University, Bologna, Italy; the [5]Endocrine-Metabolic Laboratory, Internal Medicine, Department of Medical and Surgical Sciences, Padua University, Padua, Italy; the [6]U862 Institut National de la Santé et de la Recherche Médicale, Group AVENIR, Institute François Magendie, University Bordeaux 2, Bordeaux, France; and the [7]Department of Physiological Chemistry, Johannes Gutenberg University Mainz, Mainz, Germany.

Corresponding author Enzo Nisoli, enzo.nisoli@unimi.it.

Received 16 November 2007 and accepted 7 May 2008.

Published ahead of print at http://diabetes.diabetesjournals.org on 13 May 2008. DOI: 10.2337/db07-1623.

U.P. has been a consultant for, has served on an advisory board for, and has received honoraria from sanofi-aventis. R.P. has received honoraria from sanofi-aventis.

© 2008 by the American Diabetes Association. Readers may use this article as long as the work is properly cited, the use is educational and not for profit, and the work is not altered. See http://creativecommons.org/licenses/by-nc-nd/3.0/ for details.

The costs of publication of this article were defrayed in part by the payment of page charges. This article must therefore be hereby marked "advertisement" in accordance with 18 U.S.C. Section 1734 solely to indicate this fact.

unrecognized mechanism of action for the antiobesity drug rimonabant.

RESEARCH DESIGN AND METHODS

Cell culture. White fat precursor cells were enzymatically isolated from epididymal WAT of wild-type C57BL/6J mice and cultured as described (16). SR141716 [*N*-(piperidin-1-yl)-5-(4-chlorophenyl)-1-(2,4-dichlorophenyl)-4-methylpyrazole-3-carboxamide, hydrochloride, contract no. N01-MH-32005 WA 08928.019, National Institute of Mental Health no. S-705, Chemical Synthesis and Drug Supply Program, National Institute of Mental Health; RTI)] stock solutions (50 mmol/l in DMSO) were diluted in the culture medium to the required final concentrations containing up to 0.02% DMSO. At days 3–4 from seeding, cells were exposed to the culture medium containing SR141716 (0.1–10 μmol/l) for 72 h or different periods of time when specified. The medium was discarded, the wells were washed twice with 2 ml ice-cold PBS (Sigma-Aldrich), and the cells were harvested as reported below for the different assays.

eNOS small interfering RNA. White adipocytes were transfected at days 3–4 after seeding with 100 nmol/l eNOS small interfering RNA (siRNA) SMARTpool (Dharmacon, Lafayette, CO) or *siCONTROL* nontargeting siRNA using Dharmafect 3 transfection reagent. Cells were treated for 72 h with 1 μmol/l SR141716, and RNA and protein were harvested. Efficacy of transfection was determined using si*GLO*-RISC–free nontargeting siRNA and estimation of siRNA uptake by fluorescence detection (absorbance/emission 557/570 nm).

Animals and treatments. Animals were treated according to protocols approved by Milan and Bologna University institutional animal care and use committee. Eight-week-old male CB1$^{-/-}$ mice (17) and their wild-type littermates ($n = 10$ per group) were fed either a standard mouse diet (8% kcal fat, 19% kcal protein, and 73% kcal carbohydrate) or a high-fat diet (D12492, 60% kcal fat, 20% kcal protein, and 20% kcal carbohydrate; Research Diets, New Brunswick, NJ) for 12 weeks. Moreover, 4-week-old male C57BL/6J mice (Harlan Nossan) were fed either a standard diet or high-fat diet for 6 weeks before treatments. While fed on the standard or high-fat diet, these mice ($n = 10$ per group) were further treated with either vehicle or SR141716 (at 10 mg/kg orally in distilled water with 0.1% Tween 80) for 11 weeks. Body weight and food intake were recorded weekly. Adiposity (wet weight of visceral and subcutaneous fat), cumulative food intake (for the time of the experiment), and feed efficiency were measured (5). On the day of the experiments, animals were killed by cervical dislocation and epididymal WAT was immediately isolated, frozen in liquid nitrogen, and stored at −80°C before processing for mRNA, protein, and mtDNA analysis or citrate synthase and AMP-activated protein kinase (AMPK) activity.

Isolation of mouse mature adipocytes. Wild-type and CB1$^{-/-}$ mice were fed a standard or high-fat diet ($n = 6$ per group), and wild-type mice either on standard or high-fat diet were treated with either vehicle or SR141716 ($n = 6$ per group) as described above. Mice were killed and epididymal WAT excised. Fat pads from two mice were pooled, and mature adipocytes were acutely isolated in Hank's balanced salt solution containing 4% BSA and 1.5 mg/ml collagenase (Calbiochem) as described (18).

RNA analysis. RNA was isolated from tissue or cells using the RNeasy Lipid Tissue Mini Kit (Qiagen). cDNA was synthesized using iScript cDNA Synthesis Kit (Bio-Rad Laboratories). Primers were designed using Beacon Designer 2.6 software from Premier Biosoft International. Triplicate PCR were carried out with the intercalating dye SybrGreen as previously described (5,16). PCR cycles were programmed on an iCycler iQ Real-Time PCR detection system (Bio-Rad Laboratories). The cycle number at which the various transcripts were detectable (threshold cycle [C_T]) was compared with that of β-actin, referred to as ΔC_T. The gene relative level was expressed as $2^{-(\Delta\Delta CT)}$, in which ΔΔCT equals ΔC_T of either the knockout or drug-treated mice (or treated cells) minus ΔC_T of the control mice (or untreated cells).

Immunoblot analysis. Protein extracts were obtained by harvesting cultured adipocytes in M-PER Mammalian Protein Extraction Reagent or homogenizing WAT tissue in T-PER Tissue Protein Extraction Reagent (both from Pierce), as indicated by the manufacturer, in the presence of 1 mmol/l $NaVO_4$, 10 mmol/l NaF, and a cocktail of protease inhibitors (Sigma-Aldrich). Protein content was determined by the bicinchoninic acid protein assay (Pierce), and 50 μg of proteins were run on SDS-PAGE under reducing conditions. The separated proteins were then electrophoretically transferred to a nitrocellulose membrane (Pierce). Proteins of interest were revealed with specific antibodies: anti-eNOS (Transduction Labs), anti–cytochrome c oxidase (COX IV) (Molecular Probes), anti–cytochrome c (BD Bioscience), each one at 1:500 dilution; anti–phospho-AMPKα (Thr172) and anti-AMPKα (both at 1:1,000 dilution; Cell Signaling Technology); and anti–β-actin (1:10,000; Sigma-Aldrich). The immunostaining was detected using horseradish peroxidase–conjugated anti-rabbit or anti-mouse immunoglobulin for 1 h at room temperature. After the visualization of phospho-AMPKα, filters were stripped with the Re-Blot Western blot recycling kit (Chemicon International) and further used for the visualization of total AMPKα. Bands were revealed by the SuperSignal Substrate (Pierce) and quantitated by densitometry using a Quick Image densitometer (Canberra Packard) and a Phoretix 1D, version 3.0, software image analyser.

Fluorescence-activated cell sorting analysis. White adipocytes were treated or not with 1 μmol/l SR141716 for 72 h. Cells (~1×10^6 per sample) were harvested by trypsinization, fixed with 4% paraformadehyde in PBS for 10 min, and incubated 1 h at room temperature in a permeabilization buffer containing 1% BSA, 0.1% saponin, and either anti–COX IV or anti–cytochrome c antibody. After incubation with labeled secondary antibody, the fluorescence was analyzed by flow cytometry (FACScan; Becton Dickinson, Sunnyvale, CA) and Cell Quest software (Becton Dickinson). Data are expressed as relative fluorescence intensity of the mean fluorescent signal versus unstained samples.

Mitochondrial DNA. Mitochondria were isolated from tissue and cells (19). The mitochondrial DNA (mtDNA) was extracted and analyzed as described (5,16). Briefly, an aliquot of mtDNA was loaded on ethidium bromide–stained agarose gel (1.2%) and quantified using the QuickImage densitometer (Packard). To determine mtDNA levels, the signal intensities were normalized to cell numbers in experiments on cultured cells or to protein content in experiments using tissues from wild-type and knockout mice. Alternatively, mtDNA copy number was measured by means of quantitative PCR from the cytochrome C oxidase II mtDNA gene compared with the uncoupled protein-2 nuclear gene in WAT of CB1$^{-/-}$ and wild-type mice as described (20).

Oxygen consumption. White adipocytes were harvested by trypsinization, centrifuged at 500*g* for 5 min at 4°C, and resuspended in Hank's balanced salt solution. Cell samples (4×10^6/ml) were analyzed at 37°C in a gas-tight vessel equipped with a Clark-type oxygen electrode (Rank Brothers) connected to a chart recorder. Cellular oxygen consumption was measured as described (5,16). The oxygen electrode was calibrated, assuming the concentration of oxygen in the incubation medium at 37°C to be 200 μmol/l. Protein content in both cell and tissue samples was determined by the bicinchoninic acid protein assay (Pierce).

ATP levels. The whole amount of ATP in cells was measured by using the ATP determination kit from Molecular Probes. Cells were harvested by trypsinization and centrifuged at 500*g* for 5 min at 4°C. ATP was extracted by incubating cell pellets with 1% trichloroacetic acid per 4 mmol/l EDTA solution for 10 min on ice. Cell extracts were centrifuged at 12,000*g* for 10 min at 4°C and used for ATP determination as indicated by the manufacturer.

Mitochondrial mass. White adipocytes seeded onto glass coverslips were incubated with medium containing 200 nmol/l Mitotracker red 580 (Invitrogen). After incubation for 30 min at 37°C, coverslips were rinsed two times with medium and two times with PBS and fixed at room temperature for 10 min in 4% paraformaldehyde in PBS. Coverslips were mounted onto glass slides and were then observed with a Bio-Rad confocal microscope MRC1024.

Citrate synthase activity. The activity was measured spectrophotometrically at 412 nm at 30°C in either tissue or whole-cell extracts (21). Tissue or cell homogenates were added to buffer containing 0.1 mmol/l 5,5-dithio-bis-(2-nitrobenzoic) acid, 0.5 mmol/l oxaloacetate, 50 μmol/l EDTA, 0.31 mmol/l acetyl CoA, 5 mmol/l triethanolamine hydrochloride, and 0.1 mol/l Tris-HCl, pH 8.1. Citrate synthase activity was expressed as nanomoles citrate produced per minute per milligram of protein.

AMPK assay. Adipocytes were scraped in ice-cold lysis buffer (22) in the presence of 1 mmol/l $NaVO_4$, 10 mmol/l NaF, and protease inhibitors (Sigma-Aldrich). Epididymal fat pads from wild-type or CB1$^{-/-}$ mice were homogenized in ice-cold lysis buffer. AMPK activity was determined on protein samples immunoprecipitated with anti-AMPKα (Cell Signaling Technology) as described (22). The immunocomplexes were collected and washed with AMPK reaction buffer (22). AMPK immunoprecipitates were incubated with 20 μl of AMPK reaction buffer, 5 μl of SAMS substrate peptide (1 mmol/l), and 2 μCi of [γ-^{32}P]ATP (MP Biomedicals) for 30 min at 37°C. At the end of the incubation, an aliquot was removed and spotted onto Whatman P81 paper. The P81 paper was washed three times with 0.75% (vol/vol) phosphoric acid and once with acetone, and radioactivity was determined by scintillation counting.

Statistical methods. Raw data from each experiment were analyzed using either an ANOVA with Newman-Keuls' multiple comparison post hoc test or *t* test.

RESULTS

CB1 receptor antagonist increases eNOS expression and mitochondrial biogenesis in white adipocytes.

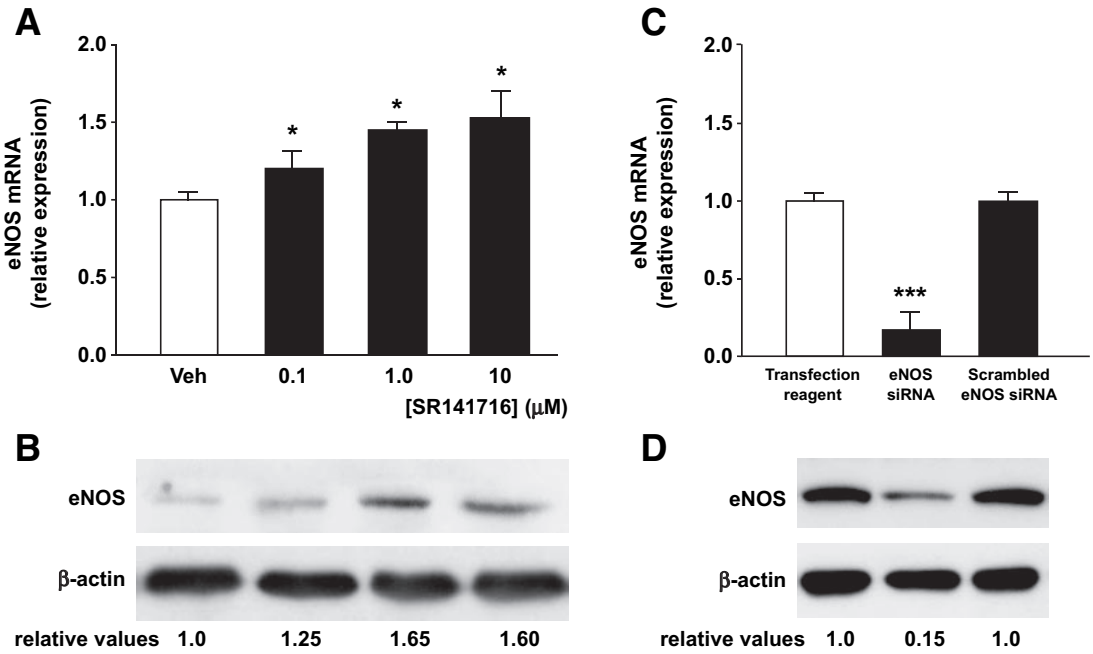

FIG. 1. The CB1 receptor antagonist SR141716 dose-dependently upregulates eNOS expression in cultured white adipocytes. *A* and *B*: eNOS mRNA and protein, analyzed by quantitative RT-PCR and immunoblotting, respectively, in vehicle-treated cells (0.02% DMSO) (Veh) or after exposure to different doses of SR141716 for 3 days. The cycle number at which the transcript was detectable was compared with that of β-actin and expressed as relative expression versus values in vehicle-treated cells taken as 1.0 ($n = 5$ experiments) (*$P < 0.05$ vs. vehicle). eNOS protein was detected by immunoblot analysis (in *B*, one experiment representative of five reproducible ones). The numbers below the blots show the relative values from the densitometric analysis, relative to β-actin levels, when control (vehicle) measurement is given a value of 1.0. *C* and *D*: eNOS expression in white adipocytes transfected with either 100 nmol/l scrambled control siRNA or eNOS siRNA and harvested 48 h later. eNOS mRNA and protein levels were measured by means of quantitative RT-PCR and immunoblotting ($n = 3$ experiments) (*$P < 0.01$ vs. transfection reagent-treated cells). All data represent means ± SE.**

CB1 receptor antagonist SR141716 affects eNOS expression in mouse white adipocytes in culture. In fact, the drug significantly increased eNOS mRNA (Fig. 1*A*) and protein levels (Fig. 1*B*) in a dose-dependent manner (0.1–10 μmol/l for 72 h).

The effect of SR141716 was further tested on several markers of mitochondrial biogenesis. The amount of mtDNA (a marker of mitochondrial content) and the mRNA levels of PGC-1α, nuclear respiratory factor-1 (NRF-1), and mtDNA transcription factor A (Tfam) (three master regulators of mitochondrial biogenesis) (23,24) were higher in 1 μmol/l SR141716-treated than in vehicle-treated cells (Fig. 2*A*). Protein levels of COX IV and cytochrome c (two mitochondrial proteins involved in oxidative phosphorylation) were also increased by SR141716 treatment as assessed either by immunoblot (Fig. 2*B*) or by flow cytometry (mean fluorescence intensity ± SE of SR141716- vs. vehicle-treated cells: 20.1 ± 3.4 vs. 9.6 ± 2.3 for COX IV and 15.6 ± 3.2 vs. 9.9 ± 1.9 for cytochrome c; $n = 3$ experiments; $P < 0.001$). Both activity of citrate synthase and oxygen consumption were markedly increased by SR141716 treatment (Fig. 2*C* and *D*). Consistently, the ATP levels in the SR141716-treated cells were significantly higher than those in the vehicle-treated cells (1.73 ± 0.19 vs. 1.34 ± 0.16; $n = 3$ experiments, $P < 0.05$). Finally, white adipocytes treated with SR141716 showed a significant increase of Mitotracker red signal, indicating the increase of mitochondrial mass compared with vehicle-treated cells (Fig. 2*E*). Altogether, these findings demonstrate that pharmacological blockade of the CB1 receptor increases eNOS expression and mitochondrial biogenesis and function in white adipocytes.

SR141716 effects on mitochondrial biogenesis are eNOS dependent. Coregulation of eNOS expression and mitochondrial biogenesis in the SR141716-treated adipocytes suggests that these processes might be mechanistically linked. To assess whether eNOS expression is relevant in the drug-induced mitochondrial biogenesis, white adipocytes were transfected with siRNA against eNOS or a scrambled RNA sequence. siRNA against eNOS reduced basal eNOS mRNA and protein levels by 82 and 85%, respectively, in WAT cells (Fig. 1*C* and *D*), with a moderate, but statistically significant, decrease of all measured parameters of mitochondrial biogenesis in vehicle-treated cells (Fig. 2*A*–*E*). Importantly, however, siRNA against eNOS strongly decreased mitochondrial biogenesis induced by 1 μmol/l SR141716 treatment, indicating that the effect of SR141716 depends, at least in part, on the presence of eNOS (Fig. 2*A*–*E*).

Mitochondrial biogenesis is increased in WAT of CB1$^{-/-}$ mice. To assess whether the CB1 receptor blockade increases mitochondrial biogenesis in WAT in vivo, we examined the eNOS expression and markers of mitochondrial biogenesis in epididymal fat pads derived from 8-week-old male CB1$^{-/-}$ mice and their wild-type littermates either on a standard or high-fat diet for 12 weeks. As expected (16), a high-fat diet reduced eNOS expression and mitochondrial biogenesis in wild-type mice (Fig. 3*A*–*D*). eNOS mRNA levels in WAT of CB1$^{-/-}$ mice were significantly higher than those of wild-type mice on both the standard and high-fat diets (Fig. 3*A*). Furthermore, CB1$^{-/-}$ mice displayed increased mRNA levels of PGC-1α and Tfam (Fig. 3*A*), COX IV, and cytochrome c (Fig. 3*C*); increased mtDNA amounts (Fig. 3*B*); and increased citrate

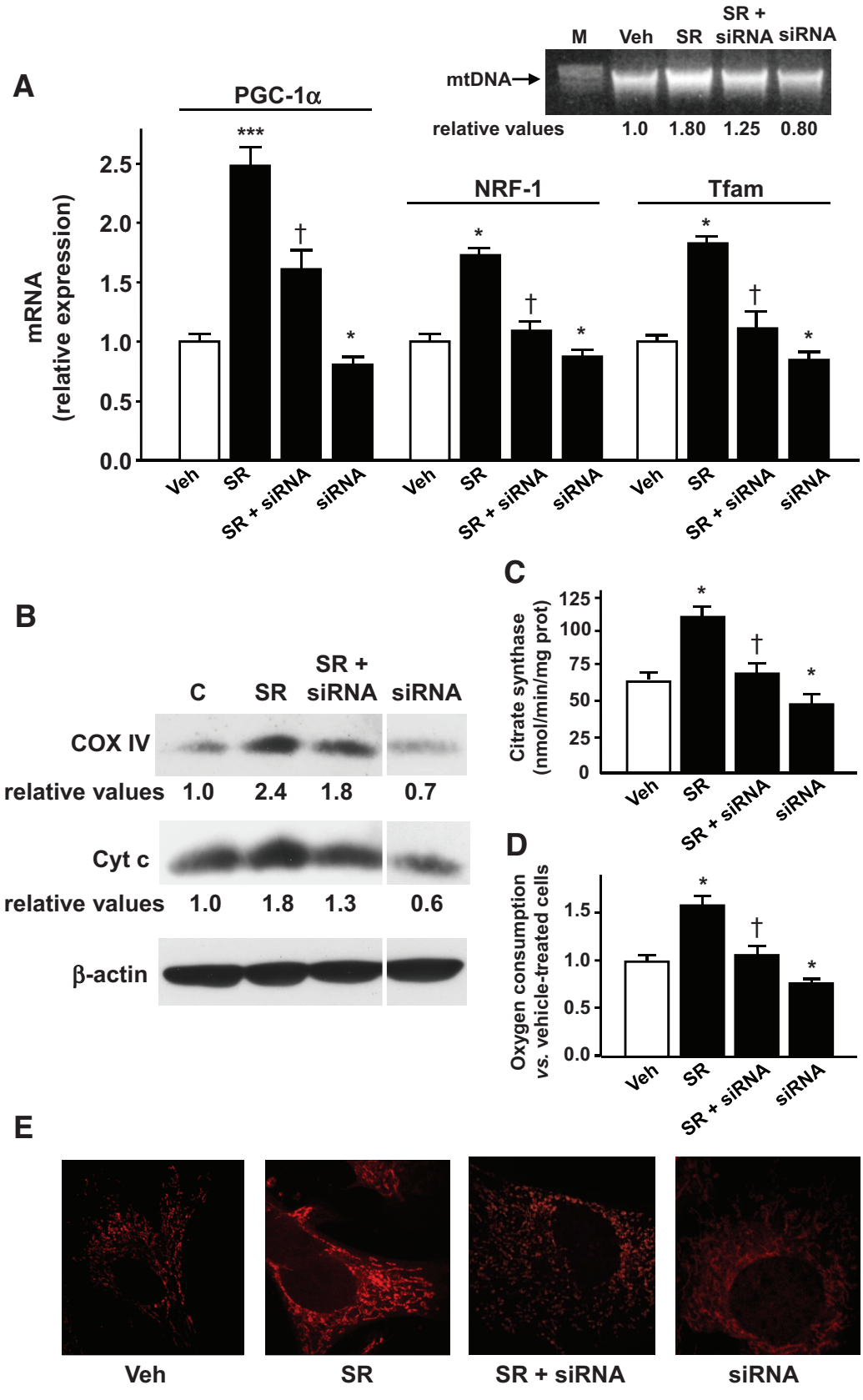

FIG. 2. SR141716 increases mitochondrial biogenesis through eNOS expression in cultured white adipocytes. *A*: PGC-1α, NRF-1, and Tfam mRNA levels were analyzed by means of quantitative RT-PCR with gene-specific oligonucleotide probes in white adipocytes treated either with vehicle (0.002% DMSO) (Veh) or 1 μmol/l SR141716 (SR) or 100 nmol/l eNOS siRNA (siRNA) either alone or combined. The cycle number at which the various transcripts were detectable was compared with that of β-actin and expressed as relative expression versus values in vehicle-treated cells taken as 1.0 (n = 5 experiments). *P < 0.05 and ***P < 0.01 vs. vehicle-treated cells; †P < 0.05 vs. SR141716-treated cells. *Inset*: mtDNA (one experiment representative of five gels). The numbers show the relative amounts from the densitometric analysis when vehicle treatment measurements are given a value of 1.0; (M, DNA marker). *B*: COX IV and cytochrome c proteins were detected by immunoblot analysis (one experiment representative of five reproducible ones) in white adipocytes. The numbers below the blots show the relative values from the densitometric analysis, referred to β-actin levels, when vehicle-treated cell measurement is given a value of 1.0. Citrate synthase activity (*C*) and oxygen consumption by white adipocytes (*D*). The values were normalized to the cell protein content (n = 3 experiments). *P < 0.05 vs. vehicle-treated cells and †P < 0.05 vs. SR141716-treated cells. All data represent means ± SE. *E*: Mitochondrial mass in white fat cells visualized as mitotracker red signal by confocal microscopy. Images were acquired by using a ×40 objective lens. (Please see http://dx.doi.org/10.2337/db07-1623 for a high-quality digital representation of this figure.)

synthase activity (Fig. 3*D*) compared with wild-type littermates. These increments were evident in animals either on standard or high-fat diets. To confirm that the mitochondrial biogenesis induced by CB1 gene deletion occurs in white adipocytes in vivo, mature white adipocytes were isolated from the epididymal fat pad of $CB1^{-/-}$ and wild-type littermates after standard or high-fat diets. Although we do not rule out that other cell types present in whole WAT (i.e., endothelial cells, macrophages, or others) may be involved, we found that CB1 gene deletion

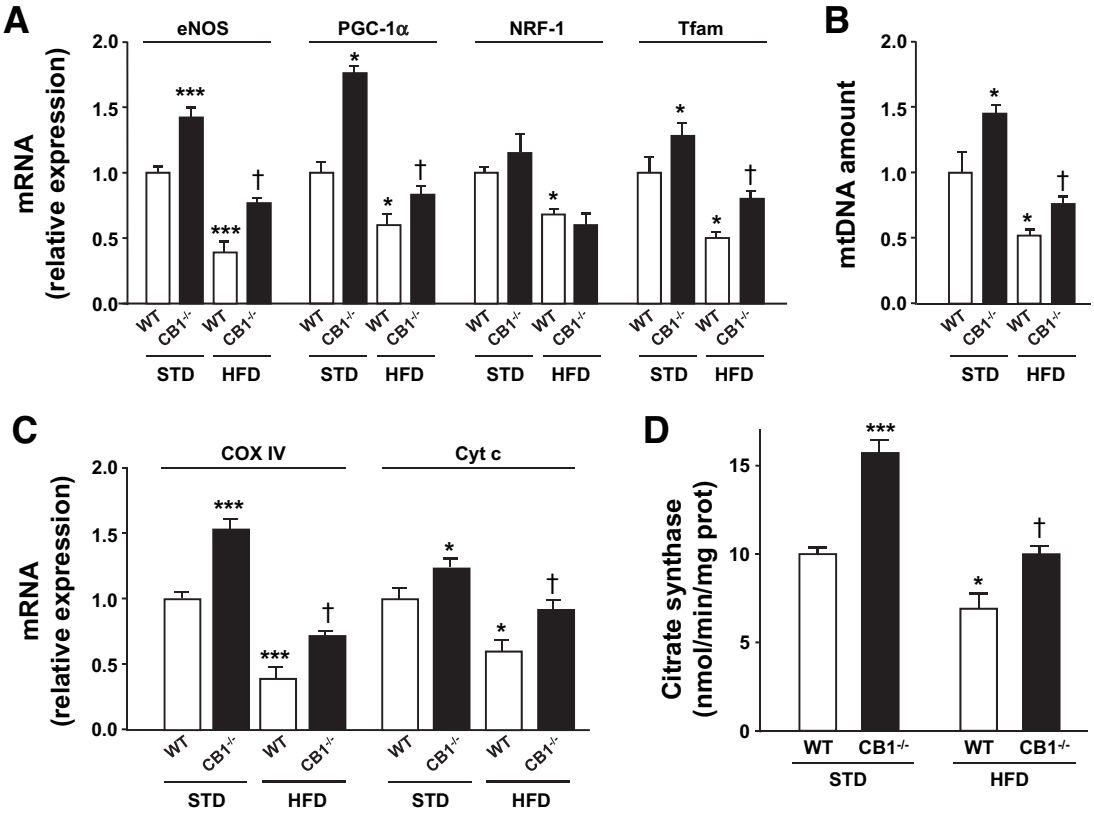

FIG. 3. Mitochondrial biogenesis is increased in WAT of CB1$^{-/-}$ mice. Eight-week-old male CB1$^{-/-}$ mice (CB1$^{-/-}$) and their wild-type (WT) littermates (n = 8 per group) were fed either a standard diet (STD) or a high-fat diet (HFD) for 12 weeks. *A* and *C*: eNOS, PGC-1α, NRF-1, Tfam, COX IV, and cytochrome c mRNA levels, analyzed by means of quantitative RT-PCR with gene-specific oligonucleotide probes. The cycle number at which the transcript were detectable was compared with that of β-actin as an internal control and expressed as relative expression versus values in wild-type animals on the standard diet taken as 1.0 (n = 8 animals) (*P < 0.05 and ***P < 0.01 vs. wild-type mice on a standard diet and †P < 0.05 vs. wild-type mice on a high-fat diet). *B*: mtDNA amount, analyzed by means of quantitative PCR and expressed as mtDNA copy number per nuclear DNA copy number. *P < 0.05 vs. wild-type mice on a standard diet and †P < 0.05 vs. wild-type mice on a high-fat diet. *D*: Citrate synthase activity normalized to WAT protein content (n = 3 experiments) *P < 0.05 and ***P < 0.01 vs. wild-type mice on a standard diet and †P < 0.05 vs. wild-type mice on a high-fat diet). All data represent means ± SE.

increases eNOS expression and mitochondrial biogenesis and function in white adipocytes (online appendix Fig. 1 [available at http://dx.doi.org/10.2337/db07-1623]).

As previously described (12), CB1$^{-/-}$ mice on the standard diet had a lower body weight and adiposity (online appendix Fig. 2*A*) than wild-type controls, having showed a significantly reduced body weight compared with wild-type mice throughout the whole period of observation (data not shown). Most importantly, CB1$^{-/-}$ mice maintained a leaner phenotype under the high-fat diet as evidenced by lower body weight and adiposity (online appendix Fig. 2*A* and *B*) (13). Cumulative food intake was comparable between the two groups of mice on standard or high-fat diet (online appendix Fig. 2*C*), although CB1$^{-/-}$ mice showed a smaller feed efficiency (weight gain/food intake, an indirect measurement of increased energy expenditure) than their wild-type littermates (online appendix Fig. 2*D*).

Defective mitochondrial biogenesis is restored in WAT of high-fat diet–fed SR141716-treated mice. CB1 receptor effects on mitochondrial biogenesis were further confirmed in vivo by a long-term treatment with the CB1 receptor antagonist. Four-week-old male mice were put on either standard or high-fat diet. Starting at week 10, standard diet– and high-fat diet–fed mice were treated either with SR141716 (10 mg · kg^{-1} day^{-1} orally) or vehicle for 11 weeks (13–15). Consistent with the data from CB1$^{-/-}$ mice, eNOS mRNA and protein levels and mitochondrial biogenesis were significantly higher in WAT of the SR141716-treated high-fat diet–fed mice than in those of vehicle-treated high-fat diet–fed mice, although as expected (16), they were lower in the vehicle-treated high-fat diet–fed mice than in the vehicle-treated standard diet–fed mice (Fig. 4). These results suggest that SR141716 treatment amends the high-fat diet–induced impairment of the NO generating system, restoring the mitochondrial function at levels observed in wild-type mice on a standard diet. Treatment with SR141716 induced only a slight, but not statistically significant, increase of eNOS expression and mitochondrial biogenesis in mice on the standard diet (Fig. 4). Superimposable results were obtained in isolated mature white adipocytes from SR141716-treated mice (online appendix Fig. 3).

Interestingly, the mean body weight and adiposity of the SR141716-treated mice were markedly lower compared with that of vehicle-treated mice on the high-fat diet (online appendix Fig. 4*A* and *B*). Cumulative food intake was comparable between the drug- and vehicle-treated animals on a high-fat diet (online appendix Fig. 4*C*), whereas SR141716-treated mice showed a reduced feed efficiency compared with their vehicle-treated high-fat diet–fed controls (online appendix Fig. 4*D*). Only slight, but not statistically significant, decreases in body weight and adiposity were seen in the SR141716-treated mice on a standard diet (online appendix Fig. 4*A* and *B*).

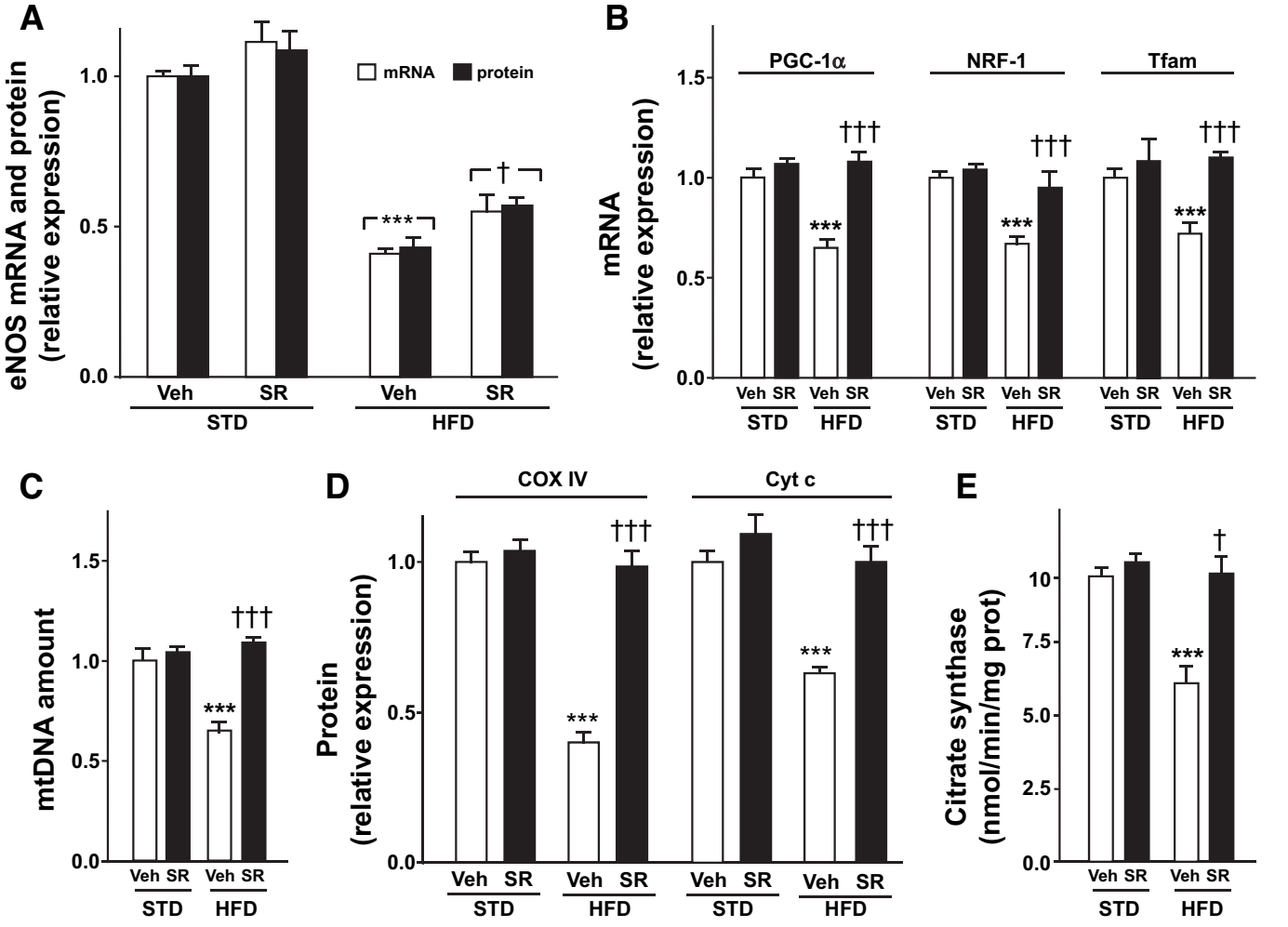

FIG. 4. eNOS expression and mitochondrial biogenesis is increased in WAT of SR141716-treated mice. Four-week-old male mice were fed either standard (STD) or high-fat (HFD) diet (n = 20 per group) for 6 weeks and were then treated either with SR141716 (10 mg · kg^{-1} · day^{-1} orally) or vehicle for 11 weeks (n = 10 per group). *A*: eNOS mRNA and protein, analyzed by quantitative RT-PCR and immunoblotting, respectively. The bars show the relative values, referred to β-actin levels, when vehicle-treated mice on standard diet measurement is given a value of 1.0. *B*: PGC-1α, NRF-1, and Tfam mRNA levels, analyzed by means of quantitative RT-PCR with gene-specific oligonucleotide probes. The bars show the relative values, referred to β-actin levels, when vehicle-treated mice on the standard diet measurement is given a value of 1.0. *C*: mtDNA amount expressed as mtDNA copy number per nuclear DNA copy number. *D*: COX IV and cytochrome c protein levels, analyzed by means of immunoblot densitometric analysis, referred to β-actin levels, when vehicle-treated mice on the standard diet measurement is given a value of 1.0. *E*: Citrate synthase activity normalized to WAT protein content (n = 3 experiments). ***P < 0.01 vs. vehicle-treated mice on a standard diet and †P < 0.05 or †††P < 0.01 vs. vehicle-treated mice on a high-fat diet. All data represent means ± SE.

CB1 receptor blockade stimulates AMPK phosphorylation and activity. The AMPK cascade has been described to activate eNOS and NO production (25). Thus, AMPK might be involved in the effect of CB1 receptor blockade on eNOS-mediated mitochondrial biogenesis. In fact, treatment of cultured white adipocytes with 1 μmol/l SR141716 induced a rapid and persistent AMPK phosphorylation (Fig. 5*A*) and significantly increased AMPK activity (Fig. 5*B*). Moreover, in line with previous reports (26), we found that AMPK activity was lower in the WAT of wild-type mice fed a high-fat diet compared with those fed a standard diet. Noticeably, while CB1 receptor deletion did not affect AMPK phosphorylation or activity in WAT of standard diet–fed mice (Fig. 5*C* and *D*), both AMPK phosphorylation (Fig. 5*C*) and activity (Fig. 5*D*) were normalized in the WAT of high-fat diet–fed CB1$^{-/-}$ mice, up to the levels measured in wild-type standard diet–fed mice.

Taken together, these findings demonstrate that the CB1 receptor blockade in vivo concomitantly activates AMPK cascade and upregulates eNOS expression and mitochondrial biogenesis, which are impaired by a high-fat diet in WAT, and these processes may be involved in the control of adiposity and body weight of animals on a high-fat diet.

DISCUSSION

The present study demonstrates that genetic and pharmacological blockade of the cannabinoid CB1 receptor increases mitochondrial biogenesis in white adipocytes. Treatment of adipocytes with SR141716, a selective antagonist of CB1 receptors (14,15,27), increases mitochondrial biogenesis genes, including PGC-1α and Tfam. This possibly implies that SR141716 is antagonizing an endocannabinoid tone present in cultured fat cells. It has been recently reported by us and others (28,29) that rodent and human adipocytes produce and release endocannabinoids, including 2-arachidonoylglycerol, anandamide, and other cannabimimetic compounds. Thus, our results suggest that SR141716 increases mitochondrial biogenesis by antago-

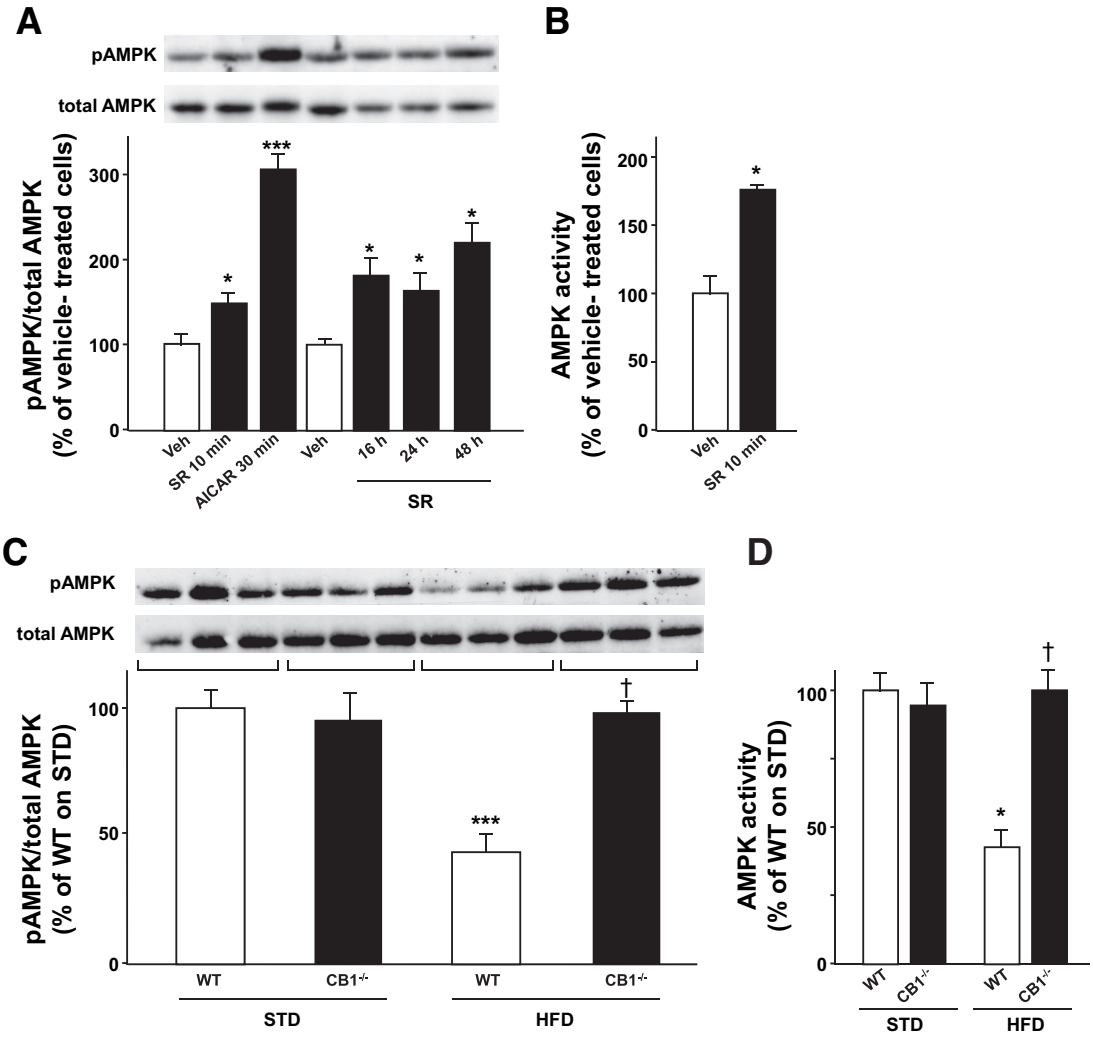

FIG. 5. AMPK phosphorylation and activity is increased by CB1 receptor blockade in vitro and in vivo. *A*: Phosphorylation of AMPK was examined in cultured white adypocytes after exposure to vehicle (0.002% DMSO) (Veh) or 1 μmol/l SR141716 for different times. 5-aminoimidazole-4-carboxamide-1-β-D-ribofuranoside (AICAR; 1 mmol/l) was used as a known inducer of AMPK phosphorylation. Western blot analyses were performed with an antibody specifically recognizing phospho-Thr172-AMPKα, then filters were stripped and reacted with an antibody recognizing both phosphorylated and unphosphorylated AMPKα. *Upper panel*: Blot images obtained from a representative experiment. *Lower panel*: Densitometric quantification of the blots from three independent cell preparations with phospho-AMPK normalized to total AMPK, when vehicle measurement is given a value of 100. *$P < 0.05$ and ***$P < 0.01$ vs. vehicle-treated cells. *B*: White adipocyte lysates were immunoprecipitated with AMPKα antibody, and the immunoprecipitates were then subjected to in vitro AMPK kinase assay. *$P < 0.05$ vs. vehicle-treated cells ($n = 3$ experiments). *C*: AMPK phosphorylation was measured in WAT protein samples from wild-type (WT) or CB1$^{-/-}$ mice fed either a standard diet (STD) or a high-fat diet (HFD). *Upper panel*: Representative immunoblots with triple protein samples from different mice. *Lower panel*: Bar graphs of densitometric quantification of the blots. ***$P < 0.01$ vs. wild-type mice on a standard diet and †$P < 0.05$ vs. wild-type mice on a high-fat diet. *D*: AMPK activity was measured as described above in epididymal WAT tissue lysates ($n = 3$ experiments) (*$P < 0.05$ vs. wild-type mice on a standard diet and †$P < 0.05$ vs. wild-type mice on a high-fat diet). All data represent means ± SE.

nizing the endocannabinoids produced in cell culture. In turn, this strongly implies that the CB1 receptor agonists might downregulate the eNOS-dependent mitochondrial biogenesis in white adipocytes. Consistently, cannabinoids, including Δ(9)-tetrahydrocannabinol, inhibit the respiratory enzyme system in brain, liver, skeletal muscle, and heart (30) and, consequently, reduce the rates of oxygen consumption in rodents (31,32).

We have recently found that eNOS-dependent NO production induces mitochondrial biogenesis in different cell types, including white adipocytes, by cGMP-dependent pathways and that the newly synthesized mitochondria are functionally active, ensuing high oxygen consumption and ATP production (5,6,33). This suggests that the SR141716-dependent increase in eNOS expression is mechanistically linked to the mitochondrial biogenesis induced by the CB1 receptor blockade. This was confirmed by the observation that gene silencing of eNOS by RNAi markedly impairs the SR141716 stimulatory effects on mitochondrial biogenesis and function in cultured adipose cells.

We observed that genetic CB1 receptor blockade in vivo increases eNOS expression and mitochondrial biogenesis both in whole WAT and isolated mature white adipocytes, and this is accompanied by prevention of high-fat diet–induced fat accumulation. Most importantly, the pharmacological CB1 receptor blockade fully counteracts the downregulation of eNOS-dependent mitochondrial biogenesis due to a high-fat diet in mice. This might indicate a novel, previously unrecognized mechanism of action of SR141716 as an antiobesity drug. Not only would it transiently suppress food intake (34,35) and reduce lipogenesis (12), but it also would increase the oxidative metabolism in white adipocytes by counteracting the inhibitory effects of endocannabinoids, whose levels are

increased in fat tissues of obese rodents and humans (28). Thus, we propose that the overactivity of endocannabinoids might contribute to downregulate mitochondrial biogenesis in white adipocytes of obese mice and that the blockade of adipose CB1 receptor might revert this process, thus preventing the high-fat diet–induced increase in adiposity and body weight gain.

There is an open question regarding the mechanisms that link CB1 receptor blockade to the eNOS expression. Furthermore, it remains to be clarified how the recovery of mitochondrial biogenesis and function in WAT could counteract the development of obesity. We found that SR141716 enhances AMPK activity in cultured white adipocytes and that the WAT AMPK activity, which is reduced by a high-fat diet, is normalized in WAT from high-fat diet–fed $CB1^{-/-}$ mice to the levels measured in wild-type standard-diet–fed mice. Since AMPK is known to enhance NO production by activating eNOS (25), the AMPK cascade might operate upstream of the NO generating system, possibly contributing to the CB1 blockade–mediated mitochondrial biogenesis. Accordingly, induction of AMPK activity has been found to increase mitochondrial content in adipocytes (36,37). Thus, the enhanced β-oxidation of free fatty acids elicited by AMPK activation (36,38) and by eNOS-dependent mitochondrial biogenesis (39) might functionally link SR141716 treatment to its antiobesity effects.

The mechanisms that link eNOS-derived NO to the gene expression machinery involved in mitochondrial biogenesis also remain to be elucidated. Studies of $eNOS^{-/-}$ mice have demonstrated an obligatory role of eNOS in mitochondrial biogenesis (5,6). Noticeably, eNOS, NO, and its intracellular messenger cGMP are located in both the cytoplasm and the nucleus, and several transcription factors possess heme moieties that can bind NO (6), but further investigation is needed to understand whether eNOS-mediated responses involve the nuclear NO/cGMP.

It is now widely accepted that obesity is causally linked to a chronic, low-grade inflammation of visceral adipose tissue, characterized by infiltrating macrophages, abnormal cytokine production, and activation of a network of inflammatory signaling pathways, including tumor necrosis factor-α and inducible NOS (iNOS) (40,41). It has been observed that upregulation of iNOS (which is induced in inflammatory conditions) often correlates with a downregulation of eNOS (16). Corroborating this, tumor necrosis factor-α increases iNOS expression in different cells and tissues, including fat (42) and inhibits eNOS expression, mitochondrial function, and energy production in WAT (16). Interestingly, SR141716 has been shown to reduce plasma tumor necrosis factor-α levels in inflammatory conditions (43). Thus, we can speculate that the anti-inflammatory effects of SR141716 could help counteracting the increase of iNOS expression and the reduction of eNOS expression and mitochondrial biogenesis in high-fat diet–induced obesity.

Endogenous cannabinoids and CB1 agonists promote vasodilation and decrease blood pressure, particularly in rodent models of hypertension (44,45). A variety of putative mechanisms could explain these effects, including the increased production of vasodilator NO in vessels. Although we have not analyzed the possible effects of SR141716 on eNOS expression in the vasculature, a recent analysis of the impact of rimonabant on blood pressure in the pooled population from four large trials with similar design (the Rimonabant-In-Obesity Program) demonstrates that there is no effect of rimonabant on blood pressure beyond the modest reduction mediated by weight loss (46).

In conclusion, our results demonstrate that mitochondrial biogenesis and function, which are impaired by a high-fat diet, are restored to normal levels in white adipocytes by the CB1 receptor antagonist SR141716, and this is accompanied by prevention of adiposity and body weight increase in high-fat–fed obese mice. In view of the present findings, targeting eNOS expression and mitochondrial biogenesis might offer therapeutic gains and simplify the drug approach to clinical situations as complex as obesity and related disorders.

ACKNOWLEDGMENTS

This work was supported by grants from the Ministero della Salute (to E.N. and M.O.C.); the Cofinanziamento 2005 Programmi di Ricerca Scientifica di Rilevante Interesse Nazionale from the Ministero dell'Istruzione, dell'Università e della Ricerca (to E.N., MOC., and R.V.); the Diabesity EC-FP6 (contract no. LSHM-CT-2003-503041) (to U.P.); Fondazione Cassa di Risparmio, Bologna, Italy (to C.C., R.P., and U.P.); Avenir Program of Institut National de la Santé et de la Recherche Médicale, in partnership with the Fondation Bettencourt Schueller (to G.M.); and the European Federation Studies of Diabetis (EFSD/Sanofi-Aventis European Programme) (to G.M. and B.L.).

We thank Clara De Palma for fluorescence-activated cell sorting analysis and Emilio Clementi for oxygen consumption measurements.

REFERENCES

1. Scherer PE: Adipose tissue: from lipid storage compartment to endocrine organ. *Diabetes* 55:1537–1545, 2006
2. Fischer-Posovszky P, Wabitsch M, Hochberg Z: Endocrinology of adipose tissue: an update. *Horm Metab Res* 39:314–321, 2007
3. Wilson-Fritch L, Burkart A, Bell G, Mendelson K, Leszyk J, Nicoloro S, Czech M, Corvera S: Mitochondrial biogenesis and remodeling during adipogenesis and in response to the insulin sensitizer rosiglitazone. *Mol Cell Biol* 23:1085–1094, 2003
4. Tanaka T, Nakatani K, Morioka K, Urakawa H, Maruyama N, Kitagawa N, Katsuki A, Araki-Sasaki R, Hori Y, Gabazza EC, Yano Y, Wada H, Nobori T, Sumida Y, Adachi Y: Nitric oxide stimulates glucose transport through insulin-independent GLUT4 translocation in 3T3–L1 adipocytes. *Eur J Endocrinol* 149:61–67, 2003
5. Nisoli E, Clementi E, Paolucci C, Cozzi V, Tonello C, Sciorati C, Bracale R, Valerio A, Francolini M, Moncada S, Carruba MO: Mitochondrial biogenesis in mammals: the role of endogenous nitric oxide. *Science* 299:896–899, 2003
6. Nisoli E, Carruba MO: Nitric oxide and mitochondrial biogenesis. *J Cell Sci* 119:2855–2862, 2006
7. Pagotto U, Marsicano G, Cota D, Lutz B, Pasquali R: The emerging role of the endocannabinoid system in endocrine regulation and energy balance. *Endocr Rev* 27:73–100, 2006
8. Matias I, Di Marzo V: Endocannabinoids and the control of energy balance. *Trends Endocrinol Metab* 18:27–37, 2007
9. Pacher P, Bátkai S, Kunos G: The endocannabinoid system as an emerging target of pharmacotherapy. *Pharmacol Rev* 58:389–462, 2006
10. Bensaid M, Gary-Bobo M, Esclangon A, Maffrand JP, Le Fur G, Oury-Donat F, Soubrié P: The cannabinoid CB1 receptor antagonist SR141716 increases Acrp30 mRNA expression in adipose tissue of obese *fa/fa* rats and in cultured adipocyte cells. *Mol Pharmacol* 63:908–914, 2003
11. Engeli S, Bohnke J, Feldpausch M, Gorzelniak K, Janke J, Batkai S, Pacher P, Harvey-White J, Luft FC, Sharma AM, Jordan J: Activation of the peripheral endocannabinoid system in human obesity. *Diabetes* 54:2838–2843, 2005
12. Cota D, Marsicano G, Tschoep M, Grubler Y, Flachskamm C, Schubert M, Auer D, Yassouridis A, Thone-Reineke C, Ortmann S, Tomassoni F, Cervino C, Nisoli E, Linthorst AC, Pasquali R, Lutz B, Stalla GK, Pagotto U:

The endogenous cannabinoid system affects energy balance via central orexigenic drive and peripheral lipogenesis. *J Clin Invest* 112:423–431, 2003
13. Ravinet Trillou C, Delgorge C, Menet C, Arnone M, Soubrié P: CB1 cannabinoid receptor knockout in mice leads to leanness, resistance to diet-induced obesity and enhanced leptin sensitivity. *Int J Obes Relat Metab Disord* 28:640–648, 2004
14. Ravinet Trillou C, Arnone M, Delgorge C, Gonalons N, Keane P, Maffrand JP, Soubrié P: Anti-obesity effect of SR141716, a CB1 receptor antagonist, in diet-induced obese mice. *Am J Physiol Regul Integr Comp Physiol* 284:R345–R353, 2003
15. Jbilo O, Ravinet-Trillou C, Arnone M, Buisson I, Bribes E, Peleraux A, Penarier G, Soubrié P, Le Fur G, Galiegue S, Casellas P: The CB1 receptor antagonist rimonabant reverses the diet-induced obesity phenotype through the regulation of lipolysis and energy balance. *FASEB J* 19:1567–1569, 2005
16. Valerio A, Cardile A, Cozzi V, Bracale R, Tedesco L, Pisconti A, Palomba L, Cantoni O, Clementi E, Moncada S, Carruba MO, Nisoli E: TNF-α down-regulates eNOS expression and mitochondrial biogenesis in fat and muscle of obese rodents. *J Clin Invest* 116:2791–2798, 2006
17. Marsicano G, Wotjak CT, Azad SC, Bisogno T, Rammes G, Cascio MG, Hermann H, Tang J, Hofmann C, Zieglgänsberger W, Di Marzo V, Lutz B: The endogenous cannabinoid system controls extinction of aversive memories. *Nature* 418:530–534, 2002
18. McClain DA, Hazel M, Parker G, Cooksey RC: Adipocytes with increased hexosamine flux exhibit insulin resistance, increased glucose uptake, and increased synthesis and storage of lipid. *Am J Physiol Endocrinol Metab* 288:E973–E979, 2005
19. Pallotti F, Lenaz G: Isolation and subfractionation of mitochondria from animal cells and tissue culture lines. In *Mitochondria*. Pon LA, Schon EA, Eds. San Diego, Academic Press, 2001, p. 1–35
20. Sparks LM, Xie H, Koza RA, Mynatt R, Hulver MW, Bray GA, Smith SR: A high-fat diet coordinately downregulates genes required for mitochondrial oxidative phosphorylation in skeletal muscle. *Diabetes* 54:1926–1933, 2005
21. Lopez-Lluch G, Hunt N, Jones B, Zhu M, Jamieson H, Hilmer S, Cascajo MV, Allard J, Ingram DK, Navas P, de Cabo R: Calorie restriction induces mitochondrial biogenesis and bioenergetic efficiency. *Proc Natl Acad Sci U S A* 103:1768–1773, 2006
22. Luo B, Parker GJ, Cooksey RC, Soesanto Y, Evans M, Jones D, McClain DA: Chronic hexosamine flux stimulates fatty acid oxidation by activating AMP-activated protein kinase in adipocytes. *J Biol Chem* 282:7172–7180, 2007
23. Handschin C, Spiegelman BM: Peroxisome proliferator-activated receptor γ coactivator 1 coactivators, energy homeostasis, and metabolism. *Endocr Rev* 27:728–735, 2006
24. Scarpulla RC: Nuclear control of respiratory gene expression in mammalian cells. *J Cell Biochem* 97:673–683, 2006
25. Morrow VA, Foufelle F, Connell JM, Petrie JR, Gould GW, Salt IP: Direct activation of AMP-activated protein kinase stimulates nitric-oxide synthesis in human aortic endothelial cells. *J Biol Chem* 278:31629–39, 2003
26. Wu Y, Song P, Xu J, Zhang M, Zou MH: Activation of protein phosphatase 2A by palmitate inhibits AMP-activated protein kinase. *J Biol Chem* 282:9777–9788, 2007
27. Gueudet C, Santucci V, Rinaldi-Carmona M, Soubrié P, Le Fur G: The CB1 cannabinoid receptor antagonist SR 141716A affects A9 dopamine neuronal activity in the rat. *Neuroreport* 6:1421–1425, 1995
28. Matias I, Gonthier MP, Orlando P, Martiadis V, De Petrocellis L, Cervino C, Petrosino S, Hoareau L, Festy F, Pasquali R, Roche R, Maj M, Pagotto U, Monteleone P, Di Marzo V: Regulation, function, and dysregulation of endocannabinoids in models of adipose and β-pancreatic cells and in obesity and hyperglycemia. *J Clin Endocrinol Metab* 91:3171–3180, 2006
29. Gonthier MP, Hoareau L, Festy F, Matias I, Valenti M, Bes-Houtmann S, Rouch C, Robert-Da Silva C, Chesne S, Lefebvre d'Hellencourt C, Cesari M, Di Marzo V, Roche R: Identification of endocannabinoids and related compounds in human fat cells. *Obesity* 15:837–845, 2007
30. Bartova A, Birmingham MK: Effect of Δ^9-tetrahydrocannabinol on mitochondrial NADH-oxidase activity. *J Biol Chem* 251:5002–5006, 1976
31. Chiu P, Karler R, Craven C, Olsen DM, Turkanis SA: The influence of Δ^9-tetrahydrocannabinol, cannabinol and cannabidiol on tissue oxygen consumption. *Res Commun Chem Pathol Pharmacol* 12:267–286, 1975
32. Pertwee RG, Tavendale R: Effects of Δ^9-tetrahydrocannabinol on the rates of oxygen consumption of mice. *Br J Pharmacol* 60:559–568, 1977
33. Nisoli E, Falcone S, Tonello C, Cozzi V, Palomba L, Fiorani M, Pisconti A, Brunelli S, Cardile A, Francolini M, Cantoni O, Carruba MO, Moncada S, Clementi E: Mitochondrial biogenesis by NO yields functionally active mitochondria in mammals. *Proc Natl Acad Sci U S A* 101:16507–16512, 2004
34. Colombo G, Agabio R, Diaz G, Lobina C, Reali R, Gessa GL: Appetite suppression and weight loss after the cannabinoid antagonist SR 141716. *Life Sci* 63:PL113–PL117, 1998
35. Simiand J, Keane M, Keane PE, Soubrié P: SR 141716, a CB1 cannabinoid receptor antagonist, selectively reduces sweet food intake in marmoset. *Behav Pharmacol* 9:179–181, 1998
36. Daval M, Foufelle F, Ferré P: Functions of AMP-activated protein kinase in adipose tissue. *J Physiol* 574:55–62, 2006
37. Orci L, Cook WS, Ravazzola M, Wang MY, Park BH, Montesano R, Unger RH: Rapid transformation of white adipocytes into fat-oxidizing machines. *Proc Natl Acad Sci U S A* 101:2058–2063, 2004
38. Matejkova O, Mustard KJ, Sponarova J, Flachs P, Rossmeisl M, Miksik I, Thomason-Hughes M, Grahame Hardie D, Kopecky J: Possible involvement of AMP-activated protein kinase in obesity resistance induced by respiratory uncoupling in white fat. *FEBS Lett* 569:245–248, 2004
39. Le Gouill E, Jimenez M, Binnert C, Jayet PY, Thalmann S, Nicod P, Scherrer U, Vollenweider P: Endothelial nitric oxide synthase (eNOS) knockout mice have defective mitochondrial β-oxidation. *Diabetes* 56: 2690–2696, 2007
40. Hotamisligil GS: Inflammation and metabolic disorders. *Nature* 444:860–867, 2006
41. Emilsson V, Thorleifsson G, Zhang B, Leonardson AS, Zink F, Zhu J, Carlson S, Helgason A, Walters GB, Gunnarsdottir S, Mouy M, Steinthorsdottir V, Eiriksdottir GH, Bjornsdottir G, Reynisdottir I, Gudbjartsson D, Helgadottir A, Jonasdottir A, Jonasdottir A, Styrkarsdottir U, Gretarsdottir S, Magnusson KP, Stefansson H, Fossdal R, Kristjansson K, Gislason HG, Stefansson T, Leifsson BG, Thorsteinsdottir U, Lamb JR, Gulcher JR, Reitman ML, Kong A, Schadt EE, Stefansson K: Genetics of gene expression and its effect on disease. *Nature* 452:423–428, 2008
42. Mérial-Kieny C, Lonchampt M, Cogé F, Verwaerde P, Galizzi JP, Boutin JA, Lafontan M, Levens N, Galitzky J, Félétou M: Endothelin-1 inhibits TNF alpha-induced iNOS expression in 3T3–F442A adipocytes. *Br J Pharmacol* 139:935–944, 2003
43. Croci T, Landi M, Galzin AM, Marini P: Role of cannabinoid CB1 receptors and tumor necrosis factor-alpha in the gut and systemic anti-inflammatory activity of SR 141716 (rimonabant) in rodents. *Br J Pharmacol* 140:115–122, 2003
44. Gebremedhin D, Lange AR, Campbell WB, Hillard CJ, Harder DR: Cannabinoid CB1 receptor of cat cerebral arterial muscle functions to inhibit L-type Ca2+ channel current. *Am J Physiol* 276:H2085–H2093, 1999
45. Bátkai S, Pacher P, Osei-Hyiaman D, Radaeva S, Liu J, Harvey-White J, Offertáler L, Mackie K, Rudd MA, Bukoski RD, Kunos G: Endocannabinoids acting at cannabinoid-1 receptors regulate cardiovascular function in hypertension. *Circulation* 110:1996–2002, 2004
46. Ruilope LM, Després JP, Scheen A, Pi-Sunyer X, Mancia G, Zanchetti A, Van Gaal L: Effect of rimonabant on blood pressure in overweight/obese patients with/without comorbidities: analysis of pooled RIO study results. *J Hypertens* 26:357–367, 2008